Notch3^{ECD} Immunotherapy Improves Cerebrovascular Responses in CADASIL Mice

Lamia Ghezali, PhD,[1] Carmen Capone, PhD,[1] Céline Baron-Menguy, PhD,[1] Julien Ratelade, PhD,[1] Søren Christensen, PhD,[2] Lars Østergaard Pedersen, PhD,[2] Valérie Domenga-Denier,[1] Jan Torleif Pedersen, PhD,[2] and Anne Joutel, MD, PhD[1,3]

Objective: CADASIL (cerebral autosomal dominant arteriopathy with subcortical infarcts and leukoencephalopathy), caused by dominant mutations in the NOTCH3 receptor, is the most aggressive small vessel disease of the brain. A key feature of its pathogenesis is accumulation of the extracellular domain of NOTCH3 receptor (Notch3^{ECD}) in small vessels, with formation of characteristic extracellular deposits termed granular osmiophilic material (GOM). Here, we investigated the therapeutic potential of a mouse monoclonal antibody (5E1) that specifically recognizes Notch3^{ECD}.

Methods: The binding affinity of 5E1 toward purified NOTCH3 was assessed using Octet analysis. The ability of 5E1 to bind Notch3^{ECD} deposits in brain vessels and its effects on disease-related phenotypes were evaluated in the CADASIL mouse model, which overexpresses a mutant rat NOTCH3. Notch3^{ECD} and GOM deposition, white matter lesions, and cerebral blood flow deficits were assessed at treatment initiation (10 weeks) and study completion (30 weeks) using quantitative immunohistochemistry, electron microscopy, and laser-Doppler flowmetry.

Results: 5E1 antibody bound recombinant rat NOTCH3 with an average affinity of 317nM. A single peripheral injection of 5E1 robustly decorated Notch3^{ECD} deposits in the brain vasculature. Chronic administration of 5E1 did not attenuate Notch3^{ECD} or GOM deposition and was not associated with perivascular microglial activation. It also failed to halt the development of white matter lesions. Despite this, 5E1 treatment markedly protected against impaired cerebral blood flow responses to neural activity and topical application of vasodilators and normalized myogenic responses of cerebral arteries.

Interpretation: This study establishes immunotherapy targeting Notch3^{ECD} as a new avenue for disease-modifying treatment in CADASIL that warrants further development.

ANN NEUROL 2018

Cadasil (cerebral autosomal dominant arteriopathy with subcortical infarcts and leukoencephalopathy) is the most common heritable cause of stroke and vascular dementia worldwide, yet there is no therapy to prevent the progression of disease manifestations. CADASIL is caused by highly stereotyped mutations that alter the number of cysteine residues in the extracellular domain of Notch3 (Notch3^{ECD}), a heterodimeric receptor predominantly expressed in blood vessels.[1,2] Several lines of evidence suggest that the toxicity of Notch3^{ECD} aggregates is a potential mechanism in CADASIL pathogenesis. Mutations alter the structure of the Notch3^{ECD} so as to promote its multimerization, extracellular accumulation, and eventual formation of granular osmiophilic material (GOM) deposits, regardless of whether they impair Notch3 receptor activity.[3,4] Notably, Notch3^{ECD} accumulation is one of the earliest pathological events in both CADASIL patients and CADASIL model mice.[5,6] Moreover, recent work has shown that mutant Notch3^{ECD} promotes the abnormal recruitment of microvascular

View this article online at wileyonlinelibrary.com. DOI: 10.1002/ana.25284

Received Oct 24, 2017, and in revised form Jun 28, 2018. Accepted for publication Jun 28, 2018.

Address correspondence to Dr Joutel, Faculté de Médecine Paris 7, 10 avenue de Verdun, Paris 75010, France. E-mail: anne.joutel@inserm.fr

From the [1]Genetics and Pathogenesis of Cerebrovascular Diseases, Inserm, Paris Diderot University, Paris, France; [2]H. Lundbeck A/S, Valby, Denmark; and [3]University Hospital Department NeuroVasc, Sorbonne Paris Cité, Paris, France

extracellular matrix proteins within GOM deposits, and that elevated levels of these proteins play a role in the disease.[4,7]

Formation of abnormal protein conformers and accumulation of protein aggregates are hallmarks of all major neurodegenerative diseases.[8] Several strategies directed at reducing the accumulation of these proteins or neutralizing their toxicity have been developed. Among these, immunotherapy has become a major focus of research, with a number of antibodies having entered human trials.[9,10]

The well-established TgNotch3^{R169C} mouse model of CADASIL recapitulates the early stage of the disease, exhibiting Notch3^{ECD}/GOM deposition, profound cerebrovascular dysfunction, and white matter lesions.[6,7] Here, we conducted a proof-of-concept study to investigate the therapeutic potential of passive immunotherapy targeting of Notch3^{ECD} in the TgNotch3^{R169C} mouse model.

Materials and Methods

Mice

TgNotch3^{R169C} mice, which overexpress a mutant rat NOTCH3 receptor containing a mutation identified in CADASIL patients, and their wild-type littermates were maintained on an FVB/N genetic background, as described previously.[6] The transgene in this line is integrated on the X chromosome, and random inactivation of 1 X chromosome in females results in mosaic expression of the mutant protein in TgNotch3^{R169C} female mice (Joutel, unpublished data). Therefore, only male mice were used in this study. All experimental procedures were approved by our local institutional animal care and use committee (Lariboisière-Villemin), and every effort was made to minimize the number of animals used.

Injected Antibodies

The 5E1 mouse monoclonal antibody (mAb; IgG1 isotype) was raised against a recombinant protein derived from epidermal growth factor repeats 17–21 (amino acids 649–847) of human NOTCH3.[1] The recombinant control mouse mAb 2H2 (isotype IgG1, hereafter termed control IgG1) was raised against the precursor peptide on an immature dengue virus.[11] The 5E1 and control IgG1 mAbs were produced by cell culture of mouse hybridoma and Chinese hamster ovary cells, respectively, in serum-free media and were purified by protein G affinity chromatography. For all antibodies, the final endotoxin concentration was <1 endotoxin units (EU/ml).

Binding Affinity

Biotinylated human and rat (amino acids 649–847) NOTCH3 proteins were produced in HEK293 human embryonic kidney cells and purified by monomeric avidin affinity chromatography. The binding affinity of 5E1 toward recombinant NOTCH3 protein was determined using Octet analysis, as previously described.[12] Briefly, protein was immobilized on streptavidin tips at a level of approximately 3 response units. Subsequent association and dissociation of 5E1 antibody were analyzed at concentrations ranging from 3.3 to 333nM. Samples were run in triplicate, and data were analyzed using ForteBio Data Analysis 7.0 software (Pall Corporation, Port Washington, NY).

5E1 Antibody Plasma Kinetics

TgNotch3^{R169C} mice (n = 20; aged 6 weeks) received a single intraperitoneal (ip) injection of 5E1 (10mg/kg body weight). Mice were randomly assigned to 5 groups (n = 4 mice/group), and blood samples were collected at the indicated time points after 5E1 injection: group 1, 15 minutes and 24 hours; group 2, 30 minutes and 48 hours; group 3, 1 and 96 hours; group 4, 4 hours and 1 week; and group 5, 8 hours and 2 weeks. 5E1 antibody levels were measured in plasma by enzyme-linked immunosorbent assay using recombinant NOTCH3 protein.

Antibody Treatment and Experimental Design

TgNotch3^{R169C} mice were randomized and dosed weekly with 5E1 or control IgG1 (10mg/kg body weight, ip) for 20 weeks, from 10 to 30 weeks of age. At the conclusion of dosing, mice were analyzed for Notch3^{ECD} load and GOM deposits in brain arteries, evoked cerebral blood flow (CBF) responses, myogenic tone of cerebral arteries, and white matter lesions in the corpus callosum. The number of mice per experimental group was determined a priori to enable detection of differences > 25 to 30% between means with 80% power ($\alpha = 0.05$) based on previously published standard deviations.[7] A parallel cohort of untreated wild-type mice was similarly analyzed at a mean age of 30 weeks, as a study completion control group. Another cohort of untreated TgNotch3^{R169C} and wild-type male mice was analyzed at a mean age of 10 weeks as a baseline group to assess the initial load of Notch3^{ECD} aggregates and white matter lesions as well as evoked CBF responses. The numbers of mice per group are indicated in figure legends. No outlier data points were removed, and all analyses were done by investigators blinded to the genotype and mAb administered.

Histology

BRAIN COLLECTION. Mice were deeply anesthetized with sodium pentobarbital (80mg/kg) and transcardially perfused with 50ml of phosphate buffer. The brain was removed, one hemisphere was immersion fixed in 4% paraformaldehyde (PFA) and processed for cryopreservation (myelin basic protein [MBP] analysis), and the second hemisphere was frozen in liquid nitrogen and stored at −80 °C until used (all other immunostaining).

IN VIVO TARGET ENGAGEMENT. Acute target engagement of 5E1 or control murine IgG1 mAbs to Notch3^{ECD} deposits was assessed by postfixing cryosections (12 μm thick) in acetone and then incubating overnight at 4 °C with rabbit polyclonal antirat Notch3^{ECD} primary antibody[7] (1:16,000). Notch3^{ECD} deposits were detected by subsequent incubation with Alexa 488–conjugated antirabbit secondary antibody (1:500; Life Technologies, Saint Aubin,

France), and murine antibody that had crossed the blood–brain barrier and engaged deposited Notch3^{ECD} was detected with Alexa 594–conjugated antimouse secondary antibody (1:500, Life Technologies). Stained sections were imaged with an SP5 confocal microscope (NeurImag imaging platform; Leica Microsystems, Centre de Psychiatrie et Neurosciences, Paris, France). Target engagement was similarly analyzed at study completion, except that an Alexa 594–conjugated antirabbit secondary antibody and an Alexa 488–conjugated antimouse secondary antibody were used.

IMMUNOHISTOCHEMISTRY. The Notch3^{ECD} deposit load was assessed by immunostaining cryosections (12 μm thick), postfixed in acetone, with rabbit polyclonal antirat Notch3^{ECD} primary antibody followed by detection with Alexa 594–conjugated antirabbit secondary antibody. Arteries were identified by immunostaining with fluorescein isothiocyanate (FITC)-conjugated anti–smooth muscle α-actin primary antibody (1:1,000, clone 1A4; Sigma-Aldrich, St Louis, MO), and capillaries were identified by immunostaining with rat monoclonal antiperlecan antibody (1:500, clone A7L6; Millipore, Molsheim, France) followed by detection with Alexa 488–conjugated antirat secondary antibody (1:500, Life Technologies). Perivascular activated microglial cells were assessed by postfixing cryosections (12 μm thick) in 4% PFA and incubating overnight at 4 °C with rat monoclonal antibody anti-CD68 (1:1,000, clone FA-11; BioRad, Marnes-la-Coquette, France), followed by detection with Alexa 594–conjugated antirat secondary antibody (1:500, Life Technologies). Arteries were identified by incubating with FITC-conjugated anti–smooth muscle α-actin primary antibody (1:1,000, clone 1A4). The myelin debris load was assessed by incubating free-floating cryosections (16 μm thick) from PFA-fixed brain tissues with mouse monoclonal anti-MBP antibody (1:7,500, SMI94; BioLegend, London, UK) followed by incubation with Alexa 594–conjugated antimouse secondary antibody. Stained sections were imaged at 20 × (MBP analysis), 40 × (analysis of CD68 and Notch3^{ECD} in capillaries), or 60 × (analysis of Notch3^{ECD} in arteries) magnification using an Eclipse 80i microscope equipped with an XYZ motorized stage (Nikon, Tokyo, Japan). Images were captured using an Andor Neo sCMOS camera and NIS Elements BR v4.0 software (Nikon), with identical settings across compared groups. The entire procedure was performed with prefixed parameters under blinded conditions.

Quantifications of Notch3^{ECD} Deposits, Myelin Debris, and Perivascular Microglial Cells

All quantitative image analyses were performed by an investigator blinded to the genotype and mAb administered, using prefixed parameters (ImageJ software, v1.49g; Fiji Distribution, National Institutes of Health, Bethesda, MD).

Notch3^{ECD} deposits were analyzed on maximal intensity projections of image stacks following a semiautomated procedure that consists of 3 main steps: (1) manual delineation of arteries on the smooth muscle α-actin channel and delineation of capillaries by automated segmentation on the perlecan channel, followed by measurement of vessel area; (2) background suppression on the Notch3^{ECD} channel using a "rolling ball" algorithm, followed by automatic detection and counting of the number of Notch3^{ECD} deposits within vessel borders using the "Find Maxima" function; and (3) segmentation on the Notch3^{ECD} channel by image thresholding, followed by automatic detection and counting of the area of Notch3^{ECD} deposits within vessel borders using the "Analyze Particles" function. Distinct sections were used to quantify deposits in arteries and capillaries. Twelve nonadjacent sections were analyzed in each mouse. The mean of 20 to 25 distinct arteries, randomly selected from 6 sections, was used to represent the Notch3^{ECD} load in arteries, and the mean of 2 randomly selected fields (416 × 351 μm) in the hippocampus per section from 6 other sections was used to represent Notch3^{ECD} load in capillaries. Results are expressed as the number and surface area of Notch3^{ECD} deposits over the vessel area.

Myelin debris spots were counted over the whole corpus callosum following a semiautomated procedure that consisted of 2 main steps: (1) a manual delineation of the corpus callosum containing the commissural fibers, followed by measurement of the corpus callosum area and mean intensity; and (2) automatic detection and counting of the number of foci within the corpus callosum borders using the "Find Maxima" function, with noise tolerance set to half the value of the mean intensity. In each mouse, 4 different sections were analyzed. Results were expressed as the number of SMI94 hyperintense foci over the area of the corpus callosum.

Perivascular microglia cells were analyzed following a semiautomated procedure that consisted of 3 main steps: (1) manual delineation of arteries on the smooth muscle α-actin channel, followed by automatic outward dilation (radius = 15 pixels) of vessel area to include perivascular cells, and measurement of the area; (2) background suppression on the CD68 channel using a "rolling ball" algorithm and thresholding; and (3) automatic detection and quantification of CD68 staining area within vessel borders using the "Analyze Particles" function. In each mouse, perivascular microglial cells were analyzed in 20 to 30 distinct arteries randomly selected from 3 sections. Results are expressed as the surface area of CD68 staining over the vessel area.

Electron Microscopy and Quantification of GOM Deposits

Ultrathin sections of the middle cerebral artery (immediately upstream of the first bifurcation) were prepared and observed under a Philips (Best, the Netherlands) CM100 electron microscope, as previously described.[6] Electron micrograph images of the artery were captured over its entire circumference using a digital camera at 7,400 × magnification (Electron Microscopy Core Facility, Institut du Fer-à-Moulin, Paris, France). Images were manually stitched using Photoshop CS6 (Adobe Systems, San Jose, CA), and the number of GOM deposits was counted on the abluminal side of smooth muscle cells. One artery was analyzed in each mouse. Image processing and quantification

were performed by an investigator blinded to the genotype and mAb administered. Results are expressed as the number of GOM deposits per 100 μm.

In Vivo Analysis of CBF Responses

Surgeries, including tracheal intubation, cannulation of the femoral artery, and craniotomy over the barrel cortex field (2 × 2 mm), were performed under anesthesia with isoflurane (maintenance, 2%) as previously described.[13] After surgery, isoflurane was gradually discontinued and anesthesia was maintained with urethane (750mg/kg) and chloralose (50mg/kg). Arterial blood pressure, blood gases, and rectal temperature were monitored and controlled (Table).

Relative CBF was monitored at the site of the cranial window using a laser-Doppler probe (Moor Instruments, Axminster, UK) positioned stereotaxically 0.5 to 1mm from the cortical surface. CBF responses were recorded after arterial pressure and blood gases had reached a steady state. The increase in CBF produced by somatosensory activation (functional hyperemia) was studied by stimulating the whiskers contralateral to the cranial window by side-to-side deflection for 1 minute. Endothelial-dependent and -independent vasodilation was studied by topical superfusion for 5 minutes of acetylcholine (10 μmol/l, Sigma-Aldrich) or adenosine (400 μmol/l, Sigma-Aldrich), respectively, dissolved in a modified Ringer solution, after which the resulting changes in CBF were monitored. CBF values were expressed as percentage increase relative to the resting level ($[CBF_{stimulus} - CBF_{resting}] / CBF_{resting}$). Zero values for CBF were obtained at the end of the experiment after the heart was stopped with an overdose of isoflurane.

Ex Vivo Analysis of Myogenic Tone

After overdosing with CO_2, mice were decapitated and their brains were harvested. Arterial segments of the posterior cerebral artery were dissected, cannulated on two glass micropipettes in an organ chamber containing physiological salt solution maintained at 37 °C (pH 7.4), and pressurized using an arteriographic system (Living Systems Instrumentation, St Albans, VT) as previously described.[13] Myogenic tone was determined by increasing intraluminal pressure from 10 to 100mmHg using a pressure-servo control pump as previously described.[13] Myogenic tone was expressed as the percentage of passive diameter ([passive diameter – active diameter] / passive diameter × 100).

Statistical Analysis

Statistical analyses were performed using GraphPad (San Diego, CA) Prism 6 software. Data are expressed as mean ± standard error of the mean. Two-group comparisons were analyzed using a 2-tailed *t* test for independent samples. Multiple comparisons were evaluated by 1-way analysis of variance (ANOVA) followed by Bonferroni post hoc test or by Kruskal-Wallis test followed by Dunn multiple comparisons test in cases where different groups did not have equal variance. Repeated-measures ANOVAs were used to compare myogenic response curves. Tests for each experiment are indicated in the figure legends. A p value < 0.05 was considered statistically significant.

Results

Characterization of 5E1 Anti-Notch3^{ECD} mAb and Study Design

We previously generated a panel of mAbs raised against human Notch3^{ECD}; among these, the 5E1 clone was found to specifically recognize NOTCH3, but not NOTCH1, NOTCH2, or NOTCH4 receptors.[1] We recently reported that the 5E1 clone could detect rat Notch3^{ECD} deposits (by immunostaining) in brain vessels of TgNotch3^{R169C} CADASIL model mice.[4,6] Prior to testing in vivo, we first determined the binding affinity of 5E1 by bio-layer interferometry technology analysis using biotinylated recombinant NOTCH3 proteins bound to streptavidin tips. The 5E1 mAb bound human NOTCH3 with an average affinity (K_D) of 68nM and rat NOTCH3 with a slightly lower affinity (K_D = 317nM).

We next assessed whether peripherally administered 5E1 was capable of entering the brain and binding vascular Notch3^{ECD} deposits. Ten-week-old TgNotch3^{R169C} mice received a single injection (ip) of 5E1 or control IgG1 mouse mAb, and immunohistochemistry was performed on the brain 72 hours later by double staining for Notch3^{ECD} deposits and injected mouse mAb using a rabbit polyclonal anti-Notch3^{ECD} antibody and an antimouse antibody, respectively. In this experiment, mice were thoroughly perfused transcardially to flush the cerebrovasculature of any remaining exogenous and endogenous antibodies before dissecting the brain, after which immunostaining was performed on acetone-fixed cryosections from unfixed brain tissue. Confocal analyses of brain sections showed that Notch3^{ECD} deposits in IgG1-injected TgNotch3^{R169C} mice were stained by the rabbit polyclonal anti-Notch3^{ECD} antibody but not by the antimouse antibody. In contrast, capillary and arterial Notch3^{ECD} deposits in 5E1-injected TgNotch3^{R169C} mice were colabeled by the rabbit polyclonal anti-Notch3^{ECD} antibody and the antimouse antibody, exhibiting a granular staining pattern typical of that observed in mice or patients with CADASIL. Notably, almost every deposit in 5E1-injected mice was decorated by the antimouse antibody, indicating that 5E1 robustly bound to brain vascular Notch3^{ECD} deposits (Fig 1).

We also conducted a pharmacokinetics study that showed that 5E1 had a median plasma half-life of 6 to 7 days in TgNotch3^{R169C} mice (data not shown).

To investigate the therapeutic potential of 5E1, we injected TgNotch3^{R169C} mice weekly with 5E1 or control IgG1 murine mAb (10mg/kg body weight) for 20 weeks. We previously reported that Notch3^{ECD} and GOM deposits are present in TgNotch3^{R169C} mice from birth and ~25 weeks of age, respectively, and documented altered CBF responses as well as white matter lesions at

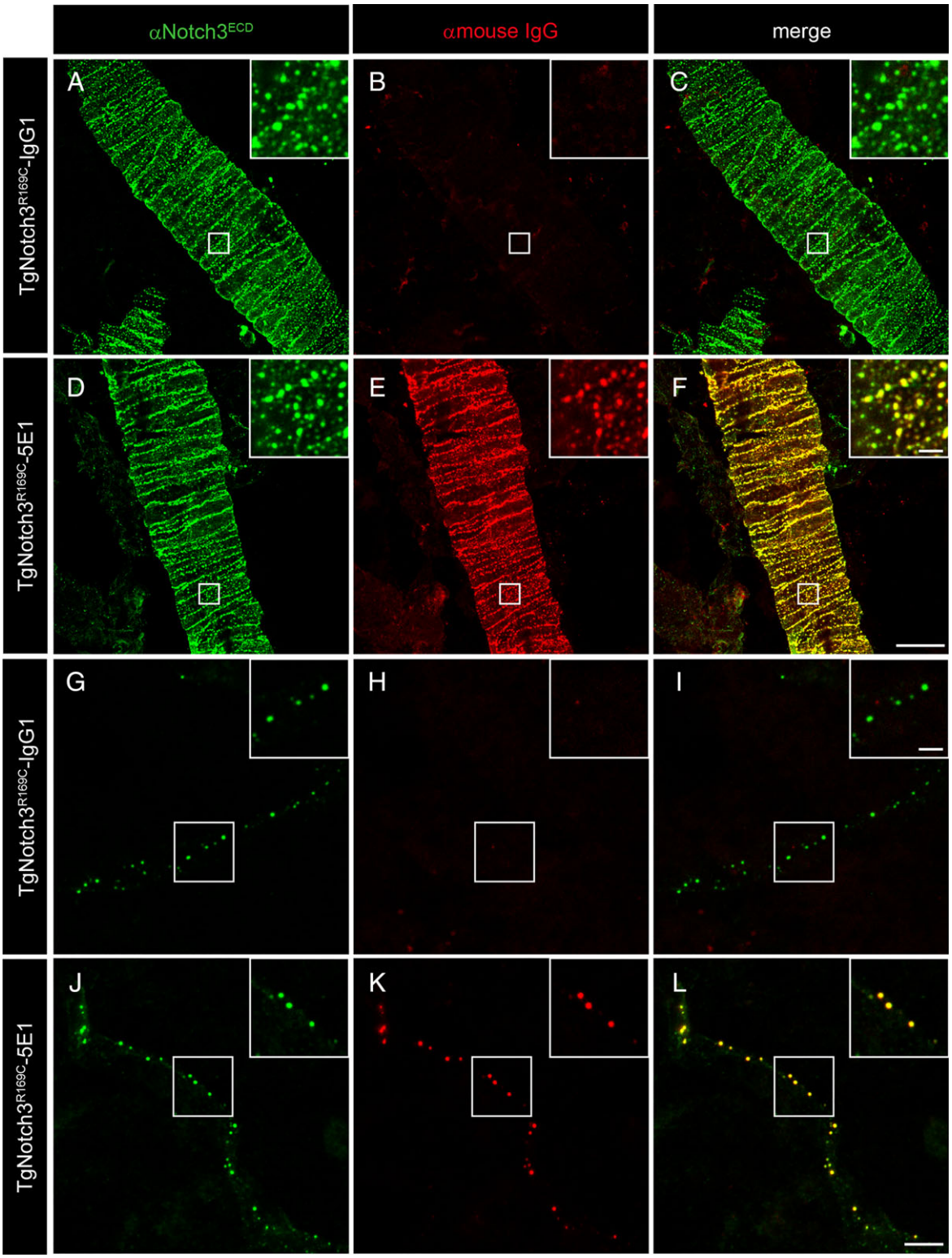

FIGURE 1: Peripherally injected 5E1 robustly engages Notch3^{ECD} deposits in brain arteries and capillaries. TgNotch3^{R169C} mice, aged 10 weeks (n = 4 mice/group), received a single 10mg/kg injection (intraperitoneal) of 5E1 (D–F, J–L) or control murine IgG1 (A–C, G–I) monoclonal antibody (mAb), and in vivo antibody target engagement was assessed 72 hours after injection. Notch3^{ECD} deposits were detected with a polyclonal antibody against Notch3^{ECD} (green; A, D, G, J), and injected murine mAbs were detected with an Alexa 594–conjugated antimouse antibody (red; B, E, H, K). Representative images of brain sections show robust decoration of Notch3^{ECD} deposits by 5E1 in arteries (D–F) and capillaries (J–L) of 5E1-injected TgNotch3^{R169C} mice and no IgG1 binding to Notch3^{ECD} deposits in arteries (A–C) or capillaries (G–I) of control IgG1-injected TgNotch3^{R169C} mice. Insets show higher magnification of boxed areas. Scale bars = 20 μm (A–F), 5 μm (G–L); for insets, 2 μm (A–L).

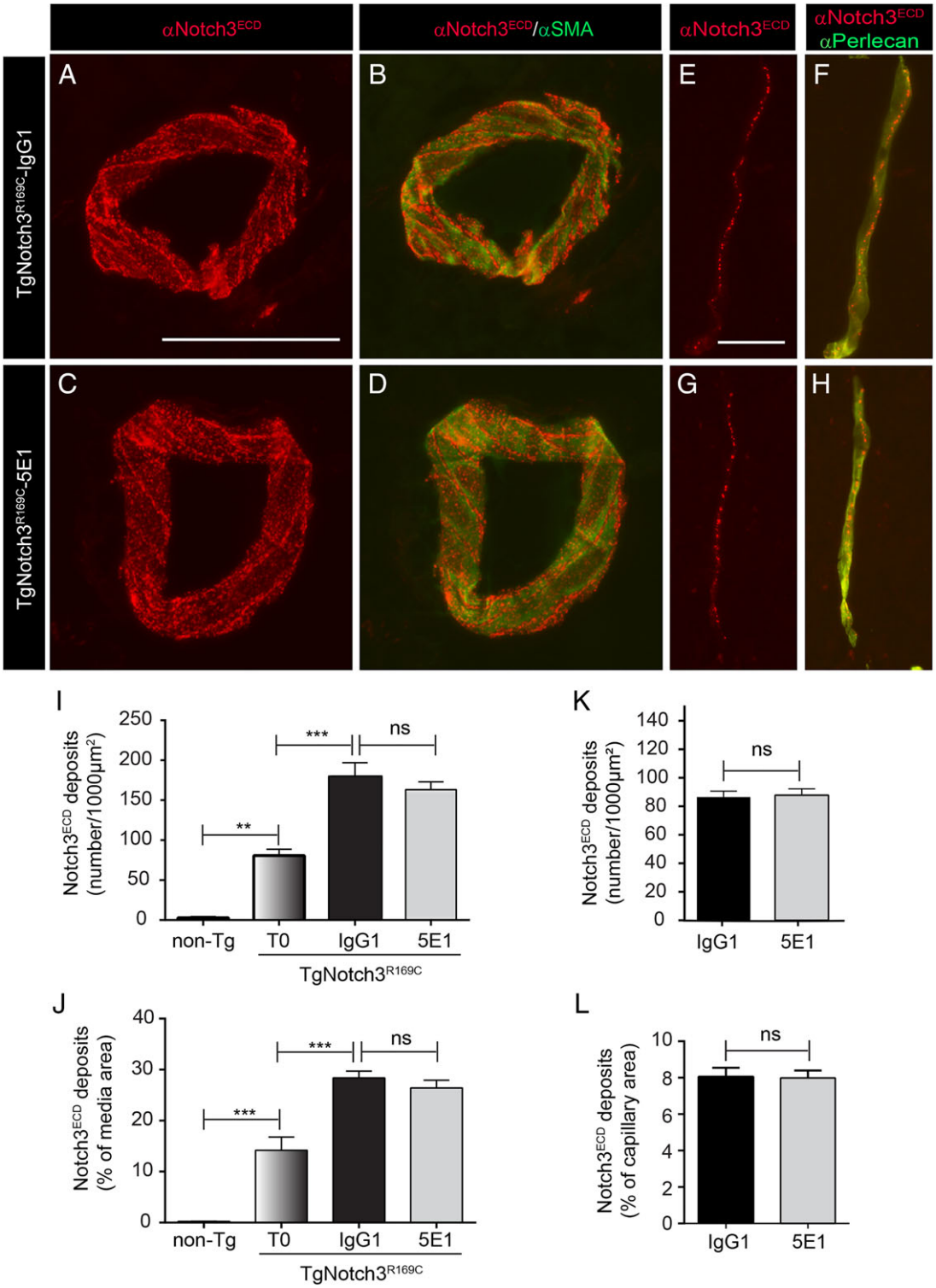

FIGURE 2: Chronic administration of 5E1 does not halt Notch3^{ECD} deposition. Notch3^{ECD} deposits were quantified in brain arteries at baseline in TgNotch3^{R169C} mice (n = 6 mice/group) and at study completion in TgNotch3^{R169C} mice treated with 5E1 or control IgG1 monoclonal antibody (mAb; n = 10 mice/group) and wild-type littermates (n = 6 mice/group). (A–H) Representative images show brain arteries (A–D) and brain capillaries (E–H) from TgNotch3^{R169C} mice treated with 5E1 (C, D, G, H) or control IgG1 mAb (A, B, E, F) stained with a polyclonal antibody against Notch3^{ECD} (red; A–H) and fluorescein isothiocyanate–conjugated anti–smooth muscle α-actin antibody (green; B, D) or antiperlecan antibody (green; F, H). (I–L) Quantification of Notch3^{ECD} deposits (numbers per 1,000 μm^2) and Notch3^{ECD} stained area revealed an increase in Notch3^{ECD} deposition from 10 to 30 weeks in brain arteries that was not decreased by 5E1 treatment (I, J). Notch3^{ECD} deposition was also comparable in brain capillaries from 5E1- and IgG1-treated mice (K, L). Significance was determined by 1-way analysis of variance followed by Bonferroni post hoc test (I, J) or Student *t* test (K, L). $^{**}p < 0.01$, $^{***}p < 0.001$; ns, not significant. Scale bars = 50 μm (A–D) and 25 μm (E–H).

~25 weeks of age.[6,7] On the basis of these observations, we treated mice from 10 to 30 weeks.

Anti-Notch3^{ECD} immunotherapy has no detectable effect on Notch3^{ECD} or GOM deposition

We first sought to determine whether 5E1 treatment attenuated Notch3^{ECD} deposition. One group of TgNotch3^{R169C} mice was sacrificed at study initiation (baseline) to determine the extent of existing Notch3^{ECD} deposits prior to dosing. Brain tissues were processed for quantitative Notch3^{ECD} immunohistochemistry, taking care to immunostain and image sections in a single batch to minimize technical variability. Quantitative analyses revealed a time-dependent accumulation of Notch3^{ECD} aggregates in the brain arteries of TgNotch3^{R169C} mice, manifesting as an almost 2-fold increase between 10 and 30 weeks (study completion). Importantly, 5E1 treatment did not affect the number or surface area of Notch3^{ECD} deposits (Fig 2A–D, I–J). Likewise, an analysis of Notch3^{ECD} load in capillaries showed no significant difference between 5E1- and IgG1-treated TgNotch3^{R169C} mice (see Fig 2E–H, K–L).

Middle cerebral arteries were also processed for quantitative electron microscopy analyses at study completion to assess GOM deposits. We found that the number of GOM deposits on the abluminal side of smooth muscle cells, where GOM deposits largely predominate, was comparable in 5E1- and control IgG1-treated mice (Fig 3A, B).

The absence of an effect of 5E1 treatment on Notch3^{ECD} and GOM deposition prompted us to assess brain vessels for histological signs of microglial/macrophage activation. A quantitative analysis showed that recruitment of CD68-positive microglial cells around brain vessels was low in 5E1-treated TgNotch3^{R169C} mice, and importantly, was not significantly different from that observed in IgG1-treated TgNotch3^{R169C} mice or age-matched wild-type mice (see Fig 3C, D). Notably, colabeling of brain sections with the rabbit polyclonal anti-Notch3^{ECD} antibody and the antimouse antibody confirmed that 5E1, but not IgG1, had robustly bound to Notch3^{ECD} deposits at study completion (see Fig 3E). Together, these data indicate that 5E1 treatment does not promote perivascular microglial activation and does not attenuate Notch3^{ECD} or GOM deposition, despite robust binding to Notch3^{ECD} deposits.

5E1 Treatment Protects against Cerebrovascular Dysfunction

We next examined whether 5E1 treatment improved CBF responses. Again, 1 group of TgNotch3^{R169C} mice was sacrificed at 10 weeks to first determine the extent of CBF deficits at baseline. We found that the increase in CBF elicited by whisker stimulation (functional hyperemia) or neocortical application of either the endothelium-dependent vasodilator acetylcholine or the smooth muscle relaxant adenosine was preserved in 10-week-old TgNotch3^{R169C} mice (Fig 4A). At the end of the study period (30 weeks), functional hyperemia and CBF responses to both vasodilators were severely impaired in control IgG1-treated TgNotch3^{R169C} mice compared with those in age-matched wild-type mice. Importantly, 5E1 treatment significantly improved functional hyperemia in TgNotch3^{R169C} mice, restoring CBF responses to a level comparable to that in wild-type mice. Likewise, CBF increases evoked by vasodilators were rescued in 5E1-treated mice (see Fig 4B).

Results from our recent studies suggest that the decrease in the myogenic tone of cerebral arteries in TgNotch3^{R169C} mice likely underlies the global cerebrovascular dysfunction exhibited by these mice.[7,13] Notably, we found that 5E1 treatment normalized myogenic tone in arteries from TgNotch3^{R169C} mice, whereas control IgG1-treated TgNotch3^{R169C} mice exhibited strongly reduced myogenic tone (see Fig 4C).

Finally, we assessed whether 5E1 treatment improved white matter lesions. PFA-fixed brain tissues were processed for quantitative immunohistochemical detection of MBP using the mouse mAb SMI94. As before, a group of TgNotch3^{R169C} mice was sacrificed at 10 weeks to determine the extent of white matter lesions at baseline. We found that cerebral white matter was unaffected in 10-week-old TgNotch3^{R169C} mice (Fig 5A, C). Because SMI94 is a mouse mAb, we next tested whether the antimouse Ab used to reveal SMI94 reacted with the 5E1 mAb bound to Notch3^{ECD} deposits under these experimental conditions. We found that almost no immunostaining of conjugated antimouse Ab was detected in PFA-fixed brain sections from 5E1-treated mice (data not shown), thus allowing reliable quantification of myelin debris, indicative of white matter lesions, in these mice. At study completion, the amount of myelin debris (spots/mm^2) in the corpus callosum was significantly increased in TgNotch3^{R169C} mice compared with age-matched wild-type mice, regardless of control IgG1 or 5E1 treatment, indicating that 5E1 had no effect on white matter lesions (see Fig 5B, D). Collectively, our results demonstrate that anti-Notch3^{ECD} treatment partially protects against cerebrovascular manifestations, but it does so without reducing Notch3^{ECD}/GOM deposition.

Discussion

Although it has been 2 decades since mutations in the NOTCH3 receptor were first identified as the cause of

CADASIL, there is still no cure for this most aggressive of all small vessel diseases. It was recently shown that an agonist Notch3 antibody that targets the heterodimerization domain of NOTCH3 and induces ligand-independent activation of the receptor partially restores the activity of a mutant NOTCH3 receptor containing a CADASIL mutation in the ligand-binding domain.[14] However, whether such an approach would be beneficial in CADASIL is

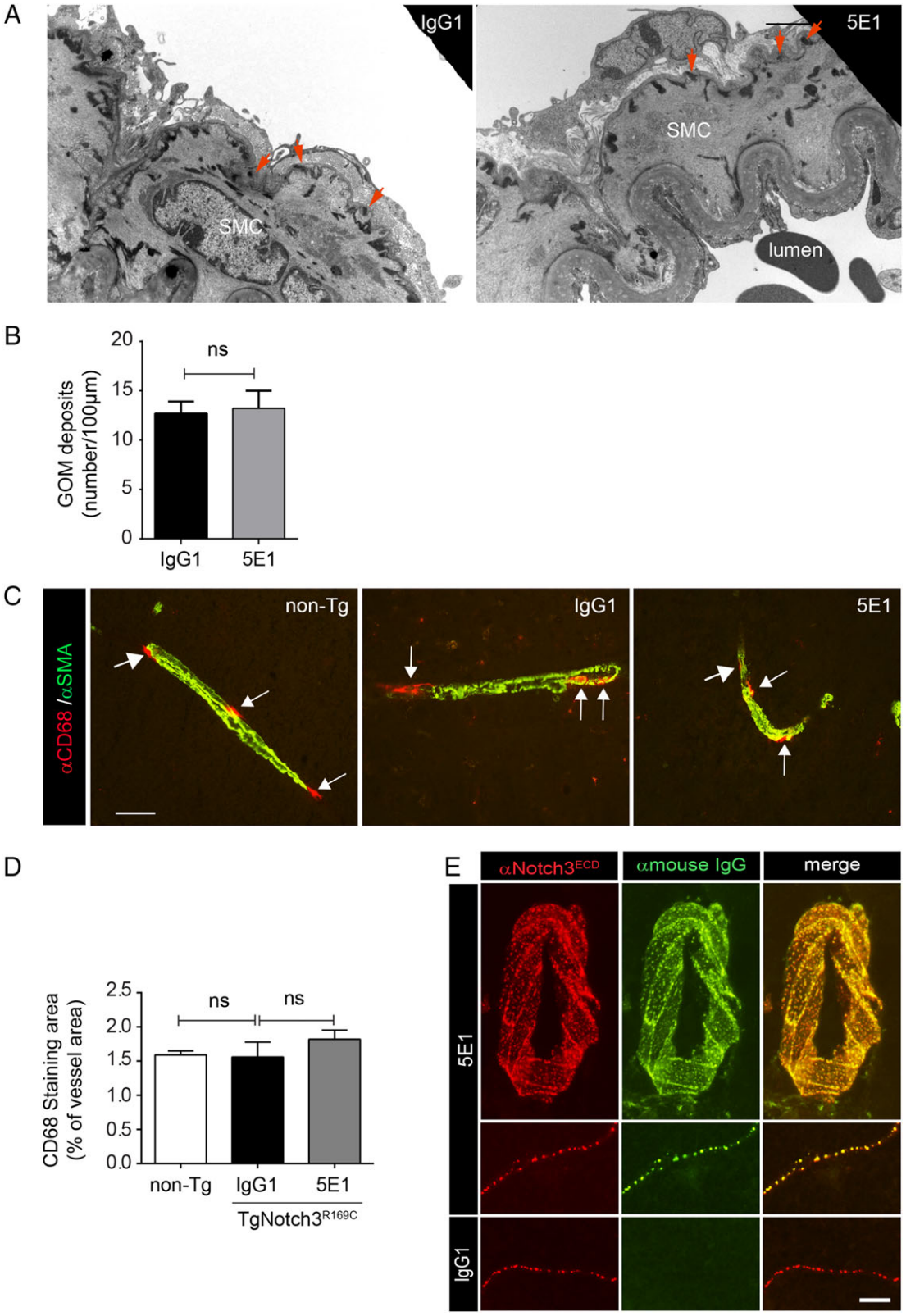

questionable, given that genetic studies in both humans and mice argue against a loss-of-function mechanism in the pathological consequences of NOTCH3 mutation.[15,16] Instead, the emerging model for the pathogenesis of CADASIL-associated NOTCH3 mutations holds that Notch3^{ECD} accumulation lies atop the cascade leading to cerebrovascular manifestations.[4] Here, we report the first evidence for the efficacy of passive immunization targeting the extracellular domain of NOTCH3 in a transgenic mouse model expressing an archetypal CADASIL mutation. We showed that a single dose of peripherally administered 5E1 robustly decorated Notch3^{ECD} deposits in the brain vasculature, despite the blood–brain barrier not being leaky at this age.[17] We further found that chronic administration of 5E1 to mutant mice protects against cerebrovascular dysfunction, normalizing functional hyperemia and vasodilatory responses as well as rescuing defects in myogenic tone.

It was rather surprising that Notch3^{ECD} immunization failed to decrease Notch3^{ECD}/GOM deposition while protecting against vascular dysfunction, especially as 5E1 treatment was initiated before Notch3^{ECD} deposition had reached a plateau. Many studies have demonstrated a reduction or even disappearance of extracellular β amyloid plaques in mouse models of Alzheimer disease following administration of antibodies against amyloid β (Aβ) peptide, whether these antibodies bind soluble or insoluble Aβ or deposited amyloid plaques.[18] Two predominant mechanisms have been proposed.[19] The first mechanism involves antibody binding to deposited amyloid plaques, with subsequent microglial/macrophage activation around plaques and phagocytosis of existing plaques.[20,21] Notably, antibodies directed against deposited amyloid have shown dose-proportional effects on plaque clearance.[21] Here, we found no evidence of perivascular microglial/macrophage activation in 5E1-treated TgNotch3^{R169C} mice, although detection of 5E1 on Notch3^{ECD} deposits following a single or multiple systemic injections confirmed that 5E1 penetrated the brain to a sufficient extent to allow accumulation on Notch3^{ECD} deposits. These observations raise the possibility that microglial function is impaired in CADASIL mice. A second mechanism, the so-called peripheral sink hypothesis, is premised on the idea that Aβ exists in a passive equilibrium between the blood and brain, and posits that soluble Aβ circulating in the blood is captured by anti-Aβ antibodies in the periphery, drawing soluble Aβ out of the brain.[22,23] However, a recent phase III trial questioned this "peripheral sink" hypothesis, showing that the humanized mAb solanezumab reduced free plasma Aβ concentration by > 90%, but failed to produce clinical efficacy.[24] A recent report suggested that Notch3^{ECD} can be detected in the plasma[25]; however, whether Notch3^{ECD} exists in a similar passive equilibrium between the brain and blood, and whether this circulating Notch3^{ECD} plays a role in brain vessel deposition, is so far unknown.

The observation that peripheral immunotherapy targeting Notch3^{ECD} protects against cerebrovascular dysfunction despite continued Notch3^{ECD} deposition and GOM formation and the absence of detectable effect on white matter lesions is particularly interesting. This leads us to revisit the concept of Notch3^{ECD}/GOM deposits as the driving force in CADASIL. Instead, mutant Notch3^{ECD} may exist in different forms, ranging from soluble species to end-stage deposits, and all potential misfolded species may contribute to the pathogenesis with potentially different biological effects. One possibility could be that soluble Notch3^{ECD} assemblies rather than aggregates represent the toxic species for cerebrovascular function, and that 5E1 antibody has cleared these soluble Notch3^{ECD} species or slowed their release from large aggregates, thereby limiting their toxic effects. Conversely, Notch3^{ECD}/GOM deposits, which have not been cleared by 5E1, could be the predominant contributors to white matter lesions. The nature of the toxic species in neurodegenerative diseases is an area of intense research. In Alzheimer disease, converging lines of evidence support

FIGURE 3: 5E1 treatment does not prevent granular osmiophilic material (GOM) deposit formation and is not associated with perivascular macrophage/microglial activation, despite robust binding to Notch3^{ECD} deposits. (A, B) GOM deposits were quantified at study completion in 30-week-old TgNotch3^{R169C} mice treated with 5E1 or control IgG1 monoclonal antibody (mAb; n = 5 mice/group). (A) Representative electron micrographs of segments of the middle cerebral artery from TgNotch3^{R169C} mice treated with 5E1 (right) or control IgG1 (left) mAb. Arrows point to GOM deposits. (B) Quantification showed that the number of GOM deposits on the abluminal side of smooth muscle cells (SMC) was comparable between 5E1- and IgG1-treated mice. (C, D) Perivascular microglial activation was assessed at study completion in 30-week-old TgNotch3^{R169C} mice treated with 5E1 or control IgG1 mAb and wild-type littermates (n = 5 mice/group). (C) Representative images show brain vessels stained with anti-CD68 antibody and fluorescein isothiocyanate–conjugated anti–smooth muscle α-actin antibody. Arrows point to CD68-positive cells. (D) Quantification of perivascular CD68-stained area shows no difference between TgNotch3^{R169C} mice treated with 5E1 or control IgG1 mAb and wild-type littermates. (E) Representative images show brain arteries (upper panel) and brain capillaries (middle and lower panels) from TgNotch3^{R169C} mice treated with 5E1 or control IgG1 mAb, stained with a polyclonal antibody against Notch3^{ECD} (red) and antimouse antibody (green), at study completion (n = 4 mice/group). Significance was determined by Student *t* test (B) or 1-way analysis of variance followed by Bonferroni post hoc test (D); ns = not significant. Scale bars = 5 μm (A), 40 μm (C), and 10 μm (E).

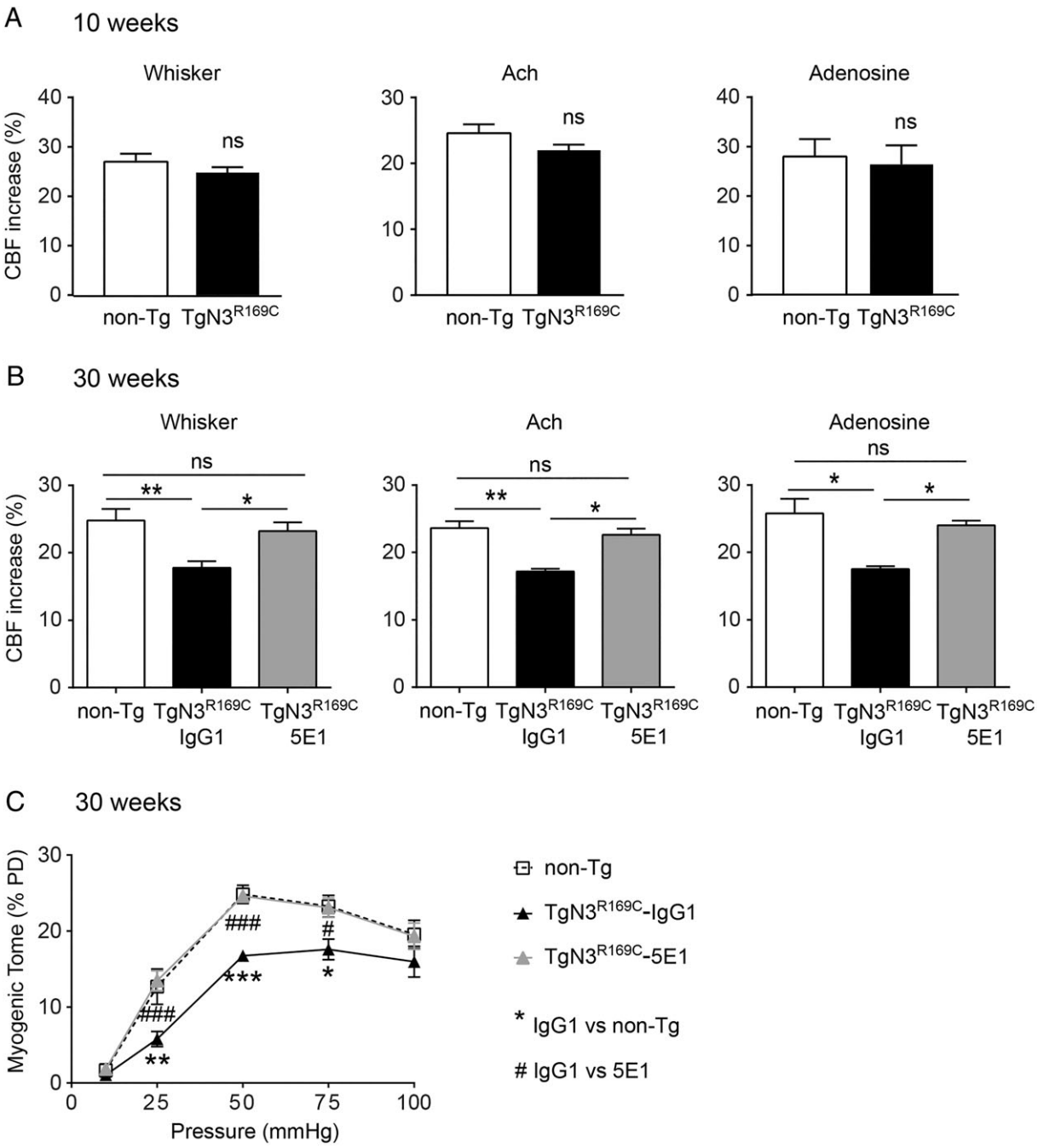

FIGURE 4: Chronic administration of 5E1 protects against cerebrovascular dysfunction in TgNotch3^{R169C} mice. (A, B) Cerebral blood flow (CBF) increases evoked by whisker stimulation, the endothelium-dependent vasodilator acetylcholine (Ach), or the smooth muscle–dependent vasodilator adenosine were analyzed at baseline in 10-week-old TgNotch3^{R169C} and wild-type littermate mice (A) and at study completion in 30-week-old TgNotch3^{R169C} treated with 5E1 or control IgG1 monoclonal antibody (mAb) and wild-type littermate mice (B; n = 5–6 mice/group). CBF responses were unaltered at baseline and were strongly attenuated at study completion in IgG1-treated mice but were rescued in 5E1-treated mice. (C) Myogenic responses of brain arteries were analyzed at study completion in 30-week-old TgNotch3^{R169C} mice treated with 5E1 or control IgG1 mAb, and in wild-type littermates. Myogenic responses were strongly reduced in IgG1-treated mice but were rescued in 5E1-treated mice (n = 7 mice/group). Significance was determined by Student *t* test (A), Kruskal-Wallis test followed by Dunn multiple comparisons test (B), or 2-way repeated measures analysis of variance followed by a Bonferroni post hoc test (C); *$p < 0.05$, **$p < 0.01$, ***$p < 0.001$, #$p < 0.05$, ###$p < 0.001$. ns = not significant; PD = passive diameter.

the concept that soluble oligomeric Aβ assemblies are the principal cytotoxic agents. Moreover, a recent report suggests that highly toxic Aβ species represent a critical minority of soluble Aβ in Alzheimer disease brain.[26] Consistent with this concept is the observation that some anti-Aβ antibodies, including oligomeric-specific antibodies, exert

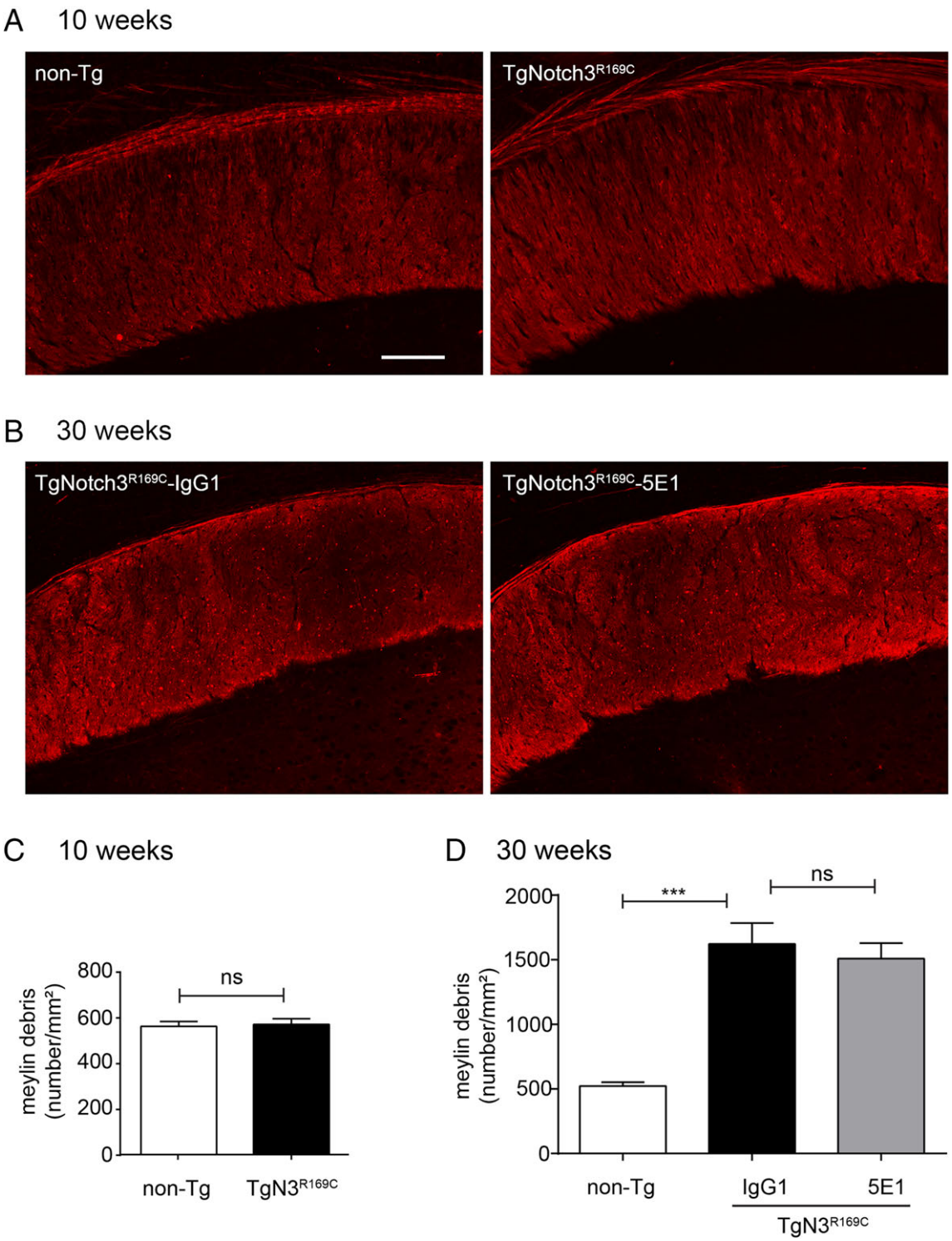

FIGURE 5: Chronic administration of 5E1 has no effect on white matter lesions in TgNotch3^{R169C} mice. Myelin debris (spots/mm^2) in the corpus callosum were quantified in free-floating brain sections immunostained with SMI94 anti–myelin basic protein antibody at baseline in 10-week-old TgNotch3^{R169C} and wild-type littermates (n = 6–7/group), and at study completion in 30-week-old TgNotch3^{R169C} mice treated with 5E1 or control IgG1 monoclonal antibody (mAb; n = 9–10 mice/group) and wild-type littermate mice (n = 6 mice/group). (A, B) Representative images of immunostaining for myelin basic protein in the corpus callosum from 10-week-old TgNotch3^{R169C} and wild-type littermates (A) and 30-week-old TgNotch3^{R169C} mice treated with 5E1 or control IgG1 mAb (B). (C, D) Quantification showed comparable numbers of myelin debris spots/mm^3 in the corpus callosum in 10-week-old TgNotch3^{R169C} and wild-type littermate mice; 30-week-old TgNotch3^{R169C} mice treated with 5E1 or control IgG1 mAb had comparable numbers of debris spots, but significantly more spots than age-matched wild-type littermates. Significance was determined by Student *t* test (C) and 1-way analysis of variance followed by Bonferroni post hoc test (D). ***$p < 0.001$; ns = not significant. Scale bar = 100 μm (A, B).

TABLE 1. Main Physiological Variables of Mice Studied in Figure 4

Genotype (Age)	n	MAP, mmHg	pCO_2, mmHg	pO_2, mmHg	pH
non-Tg (10 wk)	5	75 ± 1	35 ± 1	125 ± 3	7.35 ± 0.01
$TgNotch3^{R169C}$ (10 wk)	5	78 ± 2	35 ± 1	126 ± 2	7.35 ± 0.01
Non-Tg (30 wk)	5	79 ± 2	34 ± 1	127 ± 2	7.33 ± 0.01
$TgNotch3^{R169C}$-IgG1 (30 wk)	6	78 ± 2	34 ± 1	125 ± 2	7.33 ± 0.00
$TgNotch3^{R169C}$-5E1 (30 wk)	5	78 ± 2	34 ± 1	127 ± 2	7.34 ± 0.01

MAP = mean arterial pressure.

protective effects against synapse loss or cognitive deficits without markedly reducing the extent of plaque deposition.[27–29] Conversely, whereas several studies point toward the protective effect of aggregates by sequestering and inactivating toxic species, others suggest that aggregates themselves are disease-relevant species that can mediate a variety of pathological processes.[30] Large deposits could serve as a dynamic reservoir for the liberation of soluble oligomers.[31] Also, there is experimental evidence that aggregates can destabilize the proteostasis network by recruiting and sequestering proteins with essential cellular functions.[32] Thus, in the future, it would be important to characterize in detail all forms of $Notch3^{ECD}$ in CADASIL, to investigate the relative pathogenic importance of these different forms, and to determine whether these subspecies are modulated by passive immunization with respect to cerebrovascular pathology. However, the $TgNotch3^{R169C}$ mouse model is unlikely the appropriate paradigm for such biochemical studies. Actually, mutant NOTCH3 is overexpressed at least 4-fold in this model, and as a consequence, a significant proportion of soluble NOTCH3 protein consists of the uncleaved precursor that obscures the detection of the extracellular domain by immunoblotting (Joutel, unpublished data).

There are potential alternative mechanisms by which 5E1 may impact cerebrovascular function without having a detectable effect on white matter lesions. A recent study from our laboratory has linked cerebrovascular dysfunction and the reduction in myogenic tone of cerebral arteries to binding of deposited $Notch3^{ECD}$ to TIMP3 and subsequent elevated levels and activity of TIMP3.[7,13] 5E1 antibody binding to $Notch3^{ECD}$ deposits may have acted as a decoy to "lure" $Notch3^{ECD}$ away from interacting with TIMP3. We have attempted to analyze TIMP3 expression on brain sections using 7 different commercially available and 2 homemade anti-TIMP3 antibodies, yet we were not able to specifically detect TIMP3. Moreover, our recent data suggest that cerebrovascular dysfunction and elevated TIMP3 levels do not participate in the development of early white matter lesions, which may instead result from the binding and accumulation of other extracellular matrix protein in $Notch3^{ECD}$ deposits.[7] Hence, 5E1 might not prevent extracellular matrix proteins involved in white matter lesions from binding to $Notch3^{ECD}$.

We would like to stress that, because this was a proof-of-concept study, standard rather than optimized regimens were used. In addition, the affinity of 5E1 toward rat NOTCH3 is less than ideal. Moreover, only a very low percentage (~0.1%) of peripherally administrated antibody actually crosses the blood–brain barrier[19]—an important biological limitation of unmodified mAbs. It is also worth noting that $Notch3^{ECD}$ accumulates not only in brain vessels but also in peripheral vessels in both patients and mice with CADASIL[5] (Joutel, unpublished data). Notably, we found that peripheral vessels, such as those in the kidney, were strongly decorated by 5E1, even after a single peripheral injection (data not shown), raising the possibility that a significant proportion of peripherally injected anti-$Notch3^{ECD}$ antibody is drawn away from brain vessels.

A deficit in CBF hemodynamics is an early and important feature in both CADASIL model mice[6,33] and CADASIL patients.[2,34–36] Therefore, restoration of this functional endpoint suggests that 5E1 treatment might have beneficial effects in CADASIL patients. Nevertheless, additional studies are required before moving on to future phase I or II trials in humans. In particular, the effects of passive immunization targeting $Notch3^{ECD}$ need to be examined in preclinical studies using additional anti-$Notch3^{ECD}$ antibodies with much higher affinity toward $Notch3^{ECD}$ and replicated in mouse models expressing other CADASIL mutations. Moreover, this approach should be assessed not only in preventative studies, but also in a therapeutic setting, such as in mice with preexisting cerebrovascular manifestations. Finally, understanding the mechanism of

Notch3^{ECD} toxicity will be key to advancing the development of this therapeutic strategy. Notably, that all of our anti-Notch3^{ECD} mAbs are raised against human NOTCH3 should ease the translation of preclinical findings into clinical application.

In summary, this study identifies Notch3^{ECD} immunotherapy as a new avenue for disease-modifying treatment in CADASIL that warrants further development. Future studies addressing the mechanism of Notch3^{ECD} toxicity are needed and may support the development of more efficient anti-Notch3^{ECD} antibodies for the treatment of CADASIL.

Acknowledgment

This work was funded by H. Lundbeck A/S and supported by grants from the National Research Agency, France (ANR Genopath 2009-RAE09011HSA, ANR-16-RHUS-0004 [RHU TRT_cSVD]).

We thank S. Cleophax and E. Cognat for excellent technical assistance, and TAAM-Orleans and Paris Diderot University–site Villemin for animal housing.

Author Contributions

J.T.P. and A.J. conceived and designed the study; all authors contributed to the acquisition, analysis, and interpretation of data; AJ wrote the paper; L.G. and J.T.P., participated in drafting the article and approved the final version of the manuscript; C.C., C.B.-M., J.R., S.C., L.Ø.P., and V.D.-D. participated in revising the article and approved the final version of the manuscript.

Potential Conflicts of Interest

S.C., L.Ø.P., and J.T.P. are employees of H. Lundbeck A/S, which partially funded this study. Other authors (L.G., C.C., C.B.-M., J.R., V.D.-D., and A.J., from INSERM/University Paris 7) received neither consultant fees nor licensing payments from H. Lundbeck. INSERM/A.J. own patent rights to "Immunological treatment of cerebral autosomal dominant arteriopathy with subcortical infarcts and leukoencephalopathy," which relates to the use of antibodies against Notch3^{ECD}, including the 5E1 mAb, for treatment of CADASIL. The patent is not licensed to H. Lundbeck.

References

1. Joutel A, Andreux F, Gaulis S, et al. The ectodomain of the Notch3 receptor accumulates within the cerebrovasculature of CADASIL patients. J Clin Invest 2000;105:597–605.
2. Chabriat H, Joutel A, Dichgans M, et al. Cadasil. Lancet Neurol 2009;8:643–653.
3. Duering M, Karpinska A, Rosner S, et al. Co-aggregate formation of CADASIL-mutant NOTCH3: a single-particle analysis. Hum Mol Genet 2011;20:3256–3265.
4. Monet-Leprêtre M, Haddad I, Baron-Menguy C, et al. Abnormal recruitment of extracellular matrix proteins by excess Notch3 ECD: a new pathomechanism in CADASIL. Brain J Neurol 2013;136(pt 6): 1830–1845.
5. Joutel A, Favrole P, Labauge P, et al. Skin biopsy immunostaining with a Notch3 monoclonal antibody for CADASIL diagnosis. Lancet 2001;358:2049–2051.
6. Joutel A, Monet-Lepretre M, Gosele C, et al. Cerebrovascular dysfunction and microcirculation rarefaction precede white matter lesions in a mouse genetic model of cerebral ischemic small vessel disease. J Clin Invest 2010;120:433–445.
7. Capone C, Cognat E, Ghezali L, et al. Reducing Timp3 or vitronectin ameliorates disease manifestations in CADASIL mice. Ann Neurol 2016;79:387–403.
8. Shrivastava AN, Aperia A, Melki R, Triller A. Physico-pathologic mechanisms involved in neurodegeneration: misfolded protein-plasma membrane interactions. Neuron 2017;95:33–50.
9. Wisniewski T, Goñi F. Immunotherapeutic approaches for Alzheimer's disease. Neuron 2015;85:1162–1176.
10. Valera E, Spencer B, Masliah E. Immunotherapeutic approaches targeting amyloid-β, α-synuclein, and tau for the treatment of neurodegenerative disorders. Neurother J Am Soc Exp Neurother 2016;13: 179–189.
11. Wang Z, Li L, Pennington JG, et al. Obstruction of dengue virus maturation by Fab fragments of the 2H2 antibody. J Virol 2013;87: 8909–8915.
12. Li J, Schantz A, Schwegler M, Shankar G. Detection of low-affinity anti-drug antibodies and improved drug tolerance in immunogenicity testing by Octet(®) biolayer interferometry. J Pharm Biomed Anal 2011;54:286–294.
13. Capone C, Dabertrand F, Baron-Menguy C, et al. Mechanistic insights into a TIMP3-sensitive pathway constitutively engaged in the regulation of cerebral hemodynamics. Elife 2016;5. pii: e17536.
14. Machuca-Parra AI, Bigger-Allen AA, Sanchez AV, et al. Therapeutic antibody targeting of Notch3 signaling prevents mural cell loss in CADASIL. J Exp Med 2017;214:2271–2282.
15. Rutten JW, Boon EMJ, Liem MK, et al. Hypomorphic NOTCH3 alleles do not cause CADASIL in humans. Hum Mutat 2013;34: 1486–1489.
16. Cognat E, Baron-Menguy C, Domenga-Denier V, et al. Archetypal Arg169Cys mutation in NOTCH3 does not drive the pathogenesis in cerebral autosomal dominant arteriopathy with subcortical infarcts and leucoencephalopathy via a loss-of-function mechanism. Stroke J Cereb Circ 2014;45:842–849.
17. Ghosh M, Balbi M, Hellal F, et al. Pericytes are involved in the pathogenesis of cerebral autosomal dominant arteriopathy with subcortical infarcts and leukoencephalopathy. Ann Neurol 2015;78:887–900.
18. Golde TE, Das P, Levites Y. Quantitative and mechanistic studies of Abeta immunotherapy. CNS Neurol Disord Drug Targets 2009;8: 31–49.
19. Yu YJ, Watts RJ. Developing therapeutic antibodies for neurodegenerative disease. Neurother J Am Soc Exp Neurother 2013;10: 459–472.
20. Demattos RB, Lu J, Tang Y, et al. A plaque-specific antibody clears existing β-amyloid plaques in Alzheimer's disease mice. Neuron 2012;76:908–920.
21. Sevigny J, Chiao P, Bussière T, et al. The antibody aducanumab reduces Aβ plaques in Alzheimer's disease. Nature 2016;537:50–56.

22. DeMattos RB, Bales KR, Cummins DJ, et al. Brain to plasma amyloid-beta efflux: a measure of brain amyloid burden in a mouse model of Alzheimer's disease. Science 2002;295:2264–2267.

23. Zhang Y, Lee DHS. Sink hypothesis and therapeutic strategies for attenuating Abeta levels. Neuroscientist 2011;17:163–173.

24. Honig LS, Vellas B, Woodward M, et al. Trial of solanezumab for mild dementia due to Alzheimer's disease. N Engl J Med 2018;378: 321–330.

25. Primo V, Graham M, Bigger-Allen AA, et al. Blood biomarkers in a mouse model of CADASIL. Brain Res 2016;1644:118–126.

26. Hong W, Wang Z, Liu W, et al. Diffusible, highly bioactive oligomers represent a critical minority of soluble Aβ in Alzheimer's disease brain. Acta Neuropathol 2018;136:19–40.

27. Dorostkar MM, Burgold S, Filser S, et al. Immunotherapy alleviates amyloid-associated synaptic pathology in an Alzheimer's disease mouse model. Brain J Neurol 2014;137(pt 12):3319–3326.

28. Dodart J-C, Bales KR, Gannon KS, et al. Immunization reverses memory deficits without reducing brain Abeta burden in Alzheimer's disease model. Nat Neurosci 2002;5:452–457.

29. Lee EB, Leng LZ, Zhang B, et al. Targeting amyloid-beta peptide (Abeta) oligomers by passive immunization with a conformation-selective monoclonal antibody improves learning and memory in Abeta precursor protein (APP) transgenic mice. J Biol Chem 2006;281:4292–4299.

30. Tipping KW, van Oosten-Hawle P, Hewitt EW, Radford SE. Amyloid fibres: inert end-stage aggregates or key players in disease? Trends Biochem Sci 2015;40:719–727.

31. Winklhofer KF, Tatzelt J, Haass C. The two faces of protein misfolding: gain- and loss-of-function in neurodegenerative diseases. EMBO J 2008;27:336–349.

32. Olzscha H, Schermann SM, Woerner AC, et al. Amyloid-like aggregates sequester numerous metastable proteins with essential cellular functions. Cell 2011;144:67–78.

33. Lacombe P, Oligo C, Domenga V, et al. Impaired cerebral vasoreactivity in a transgenic mouse model of cerebral autosomal dominant arteriopathy with subcortical infarcts and leukoencephalopathy arteriopathy. Stroke 2005;36:1053–1058.

34. Liem MK, Lesnik Oberstein SA, Haan J, et al. Cerebrovascular reactivity is a main determinant of white matter hyperintensity progression in CADASIL. AJNR Am J Neuroradiol 2009;30:1244–1247.

35. Moreton FC, Cullen B, Delles C, et al. Vasoreactivity in CADASIL: comparison to structural MRI and neuropsychology. J Cereb Blood Flow Metab 2018;38:1085-1095.

36. Huneau C, Houot M, Joutel A, et al. Altered dynamics of neurovascular coupling in CADASIL. Ann Clin Transl Neurol 2018;5:788–802.